# 21

# Geometric Methods for Multirobot Optimal Motion Planning

Calin Belta[1] and Vijay Kumar[2]

[1] Mechanical Engineering and Mechanics, Drexel University, Philadelphia, PA
calin@drexel.edu
[2] GRASP Laboratory, University of Pennsylvania, Philadelphia, PA,
kumar@grasp.cis.upenn.edu

## 21.1 Introduction

As a result of technological advances in control techniques for single vehicles and the explosion in computation and communication capabilities, the interest in cooperative robotics has dramatically increased in the last few years. The research in the field of control and coordination for multiple robots is currently progressing in areas like automated highway systems [34], formation flight control [2], unmanned underwater vehicles [29], satellite clustering [22], exploration [7], surveillance [15], search and rescue, mapping of unknown or partially known environments, distributed manipulation [21], and transportation of large objects [31].

There are roughly three approaches to multivehicle coordination reported in literature: leader following, behavioral methods, and virtual structure techniques. In leader following, some robots are designated as leaders, while others are followers [10]. In behavior-based control [1] several desired behaviors are prescribed for each agent, the final control being derived by weighting the relative importance of each behavior. In the virtual structure approach, the entire formation is treated as a rigid body [13, 19, 24]. Desired motion is assigned to the virtual structure that traces out trajectories for each member of the formation to follow.

Virtual structures, as rigid bodies, evolve on the Lie group of all translations and orientations in 3D, $SE(3)$. The problem of finding a smooth interpolating curve is well understood in Euclidean spaces [14], but it is not clear how these techniques can be generalized to curved spaces. There are two main issues that need to be addressed. First, it is desired that the computational scheme be independent of the description of the space and invariant with respect to the choice of the coordinate systems used to describe the motion. Second, the smoothness properties and the optimality of the trajectories need to be considered. Shoemake [28] proposed a scheme for interpolating rotations with Bezier curves based on the spherical analog of the de Casteljau

algorithm. This idea was extended by Park and Ravani [25] to spatial motions. Another class of methods is based on the representation of Bezier curves with Bernstein polynomials. Ge and Ravani [16] used the dual unit quaternion representation of $SE(3)$ and subsequently applied Euclidean methods to interpolate in this space. Srinivasan [30] and Jütler [18] propose the use of spatial rational B-splines for interpolation. Marthinsen [20] suggests the use of Hermite interpolation and the use of truncated inverse of the differential of the exponential mapping and the truncated Baker–Campbell–Hausdorff formula to simplify the construction of interpolation polynomials. The advantage of these methods is that they produce rational curves. It is worth noting that all these works (with the exception of [25]) use a particular parameterization of the group and do not discuss the invariance of their methods. In contrast, Noakes et al. [23] derived the necessary conditions for cubic splines on general manifolds without using a coordinate chart. These results are extended in [9] to the dynamic interpolation problem. Necessary conditions for higher-order splines are derived in Camarinha et al. [8]. A coordinate-free formulation of the variational approach was used to generate shortest paths and minimum acceleration and jerk trajectories on $SO(3)$ and $SE(3)$ in [36]. However, analytical solutions are available only in the simplest of cases, and the procedure for solving optimal motions, in general, is computationally intensive. If optimality is sacrificed, it is possible to generate bi-invariant trajectories for interpolation and approximation using the exponential map on the Lie algebra [35]. While the solutions are of closed form, the resulting trajectories have no optimality properties.

Most of the existing works on motion planning and control of virtual structures use formation graphs, whose nodes capture the individual agent kinematics or dynamics, and edges represent interagent constraints that must be satisfied [10, 32, 33]. The notions of graph rigidity, minimally rigid graphs, and node augmentation are studied and applied to formations by Olfati-Saber and Murray [24] and Eren and Morse [13]. Stabilization of a formation at a given rigid configuration is formulated in terms of a structural potential function [24] or a formation function [12]. An alternative to constructing structural potential functions induced by formation graphs and a relaxation to the rigidity constraint is to use biologically inspired *artificial potential functions*, as Leonard and Fiorelli suggest in [19]. Along different lines, a geometric formulation of feasibility on formation graphs is given by Tabuada et al. [32].

We first describe a method to generate smooth trajectories for a rigid body with specified boundary conditions. The method involves two key steps: (1) the generation of optimal trajectories in $GA^+(n)$, a subgroup of the affine group in $\mathbb{R}^n$; (2) the projection of the trajectories onto $SE(3)$, the Lie group of rigid body displacements. The overall procedure is invariant with respect to both the local coordinates on the manifold and the choice of the inertial frame. The benefits of the method are threefold. First, it is possible to apply any of the variety of well-known, efficient techniques to generate optimal curves on $GA^+(n)$. Second, the method yields approximations to optimal so-

lutions for general choices of Riemannian metrics on $SE(3)$. Third, from a computational point of view, the method we propose is less expensive than traditional methods.

These results are then extended to generate motion plans for fully actuated robots required to maintain a rigid structure. The fundamental idea is based on the definition of a kinetic energy metric in the configuration space of the team. We decompose the kinetic energy into two terms: the first corresponds to the motion of a rigid structure, and the second to motions that violate the rigidity constraint. The first set of motions can be associated to orbits of the Euclidean group, $SE(3)$ or $SE(2)$. The second corresponds to velocity vectors that are orthogonal to the first. The kinetic energy metric is "shaped" by assigning different weights to each contribution. This idea of a "decomposition" and a subsequent "modification" is related to the methodology of controlled Lagrangians described in [6]. The geodesic flow for this modified metric is derived, and trajectories of the individual robots are generated. When the weights are biased toward the rigid body motion, the obtained trajectories correspond to optimal rigid body motions in 3D space ($SE(3)$) or in the plane ($SE(2)$). Other choices of weights lead to the special cases of the robots moving toward each other or each individual robot traversing its own optimal path.

The remainder of this chapter is organized as follows. Section 21.2 is a short overview of the differential geometry tools that are used in this work. Section 21.3 describes a computationally efficient, left-invariant method for generating smooth trajectories for a moving rigid body with specified boundary conditions. Smooth trajectories for a set of mobile robots satisfying constraints on relative positions are generated in Sect. 21.4. The paper concludes with final remarks and directions of future work in Sect. 21.5.

## 21.2 The Geometry of Rigid Body Motion

This section is a short review of the mathematical tools that are used in this chapter. The reader interested in a more detailed description is referred to [11].

### 21.2.1 Matrix Lie Groups and Rigid Motion

Let $GL^+(n)$ denote the set of all $n \times n$ real matrices with positive determinant:

$$GL^+(n) = \left\{ M \,|\, M \in \mathbb{R}^{n \times n},\, \det M > 0 \right\}. \tag{21.1}$$

$SO(n)$ is a subset of $GL^+$, defined as

$$SO(n) = \left\{ R \,|\, R \in GL^+(n),\, RR^{\mathrm{T}} = I \right\}. \tag{21.2}$$

Let

$$GA^+(n) = \left\{ B \,|\, B = \begin{bmatrix} M & d \\ 0 & 1 \end{bmatrix},\, M \in GL^+(n),\, d \in \mathbb{R}^n \right\}, \tag{21.3}$$

and

$$SE(n) = \left\{ A \,|\, A = \begin{bmatrix} R & d \\ 0 & 1 \end{bmatrix},\, R \in SO(n),\, d \in \mathbb{R}^n \right\}. \tag{21.4}$$

$GL^+(n)$, $SO(n)$, $GA^+(n)$, and $SE(n)$ have the structure of a group under matrix multiplication. Moreover, matrix multiplication and inversion are both smooth operations, which make all $GL^+(n)$, $SO(n)$, $GA^+(n)$, and $SE(n)$ Lie groups [11].

$GL^+(n)$ and $GA^+(n)$ are subgroups of the general linear group $GL(n)$ (the set of all nonsingular $n \times n$ matrices) and of the affine group $GA(n) = GL(n) \times \mathbb{R}^n$, respectively. $SO(n)$ is referred to as the special orthogonal group or the rotation group on $\mathbb{R}^n$. The special Euclidean group $SE(n)$ is the set of all rigid displacements in $\mathbb{R}^n$.

Special consideration will be given to $SO(3)$ and $SE(3)$. Consider a rigid body moving in free space. Assume any inertial reference frame $\{F\}$ fixed in space and a frame $\{M\}$ fixed to the body at point $O'$ ( Fig. 21.1). At each instance the configuration (position and orientation) of the rigid body can be described by a homogeneous transformation matrix, $A \in SE(3)$, corresponding to the displacement from frame $\{F\}$ to frame $\{M\}$.

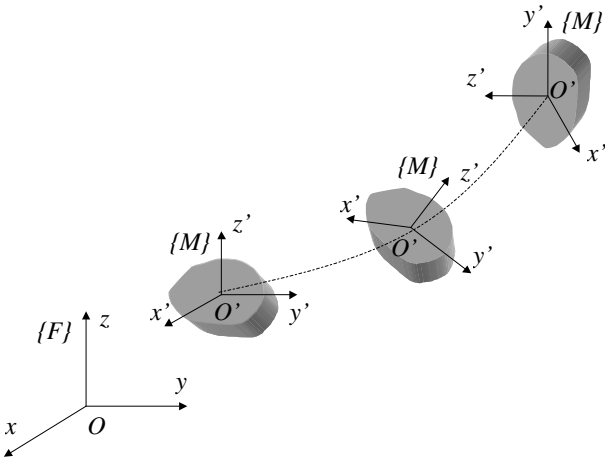


**Fig. 21.1.** The inertial (fixed) frame and the moving frame attached to the rigid body

On any Lie group the tangent space at the group identity has the structure of a Lie algebra. The Lie algebras of $SO(3)$ and $SE(3)$, denoted by $so(3)$ and $se(3)$, respectively, are given by:

$$so(3) = \left\{ \hat{\omega} \,|\, \hat{\omega} \in \mathbb{R}^{3\times 3},\ \hat{\omega}^{\mathrm{T}} = -\hat{\omega} \right\}, \tag{21.5}$$

$$se(3) = \left\{ S = \begin{bmatrix} \hat{\omega} & v \\ 0 & 0 \end{bmatrix} \ | \ \hat{\omega} \in so(3), v \in \mathbb{R}^3 \right\}, \tag{21.6}$$

where $\hat{}$ is the skew-symmetric operator.

Given a curve

$$A(t) : [-a, a] \to SE(3),\ A(t) = \begin{bmatrix} R(t) & d(t) \\ 0 & 1 \end{bmatrix},$$

an element $S(t)$ of the Lie algebra $se(3)$ can be identified with the tangent vector $\dot{A}(t)$ at an arbitrary point $t$ by:

$$S(t) = A^{-1}(t)\dot{A}(t) = \begin{bmatrix} \hat{\omega}(t) & R^{\mathrm{T}}\dot{d} \\ 0 & 0 \end{bmatrix}, \tag{21.7}$$

where $\hat{\omega}(t) = R(t)^{\mathrm{T}}\dot{R}(t)$ is the corresponding element from $so(3)$.

A curve on $SE(3)$ physically represents a motion of the rigid body. If $\{\omega(t), v(t)\}$ is the vector pair corresponding to $S(t)$, then $\omega$ physically corresponds to the angular velocity of the rigid body, while $v$ is the linear velocity of the origin $O'$ of the frame $\{M\}$, both expressed in the frame $\{M\}$. In kinematics, elements of this form are called twists, and $se(3)$ thus corresponds to the space of twists. The twist $S(t)$ computed from Eq. (21.7) does not depend on the choice of the inertial frame $\{F\}$ and is therefore called left invariant.

The standard basis for the vector space $so(3)$ is:

$$L_1^o = \hat{e}_1,\ L_2^o = \hat{e}_2,\ L_3^o = \hat{e}_3, \tag{21.8}$$

where

$$e_1 = \begin{bmatrix} 1\ 0\ 0 \end{bmatrix}^{\mathrm{T}},\ e_2 = \begin{bmatrix} 0\ 1\ 0 \end{bmatrix}^{\mathrm{T}},\ e_3 = \begin{bmatrix} 0\ 0\ 1 \end{bmatrix}^{\mathrm{T}}.$$

$L_1^o$, $L_2^o$, and $L_3^o$ represent instantaneous rotations about the Cartesian axes $x$, $y$, and $z$, respectively. The components of a $\hat{\omega} \in so(3)$ in this basis are given precisely by the angular velocity vector $\omega$.

The standard basis for $se(3)$ is:

$$\begin{gathered} L_1 = \begin{bmatrix} L_1^o & 0 \\ 0 & 0 \end{bmatrix}\ L_2 = \begin{bmatrix} L_2^o & 0 \\ 0 & 0 \end{bmatrix}\ L_3 = \begin{bmatrix} L_3^o & 0 \\ 0 & 0 \end{bmatrix} \\ L_4 = \begin{bmatrix} 0 & e_1 \\ 0 & 0 \end{bmatrix}\ L_5 = \begin{bmatrix} 0 & e_2 \\ 0 & 0 \end{bmatrix}\ L_6 = \begin{bmatrix} 0 & e_3 \\ 0 & 0 \end{bmatrix} \end{gathered} \tag{21.9}$$

The twists $L_4$, $L_5$, and $L_6$ represent instantaneous translations along the Cartesian axes $x$, $y$, and $z$, respectively. The components of a twist $S \in se(3)$ in this basis are given precisely by the velocity vector pair $s := \{\omega, v\} \in \mathbb{R}^6$.

### 21.2.2 Riemannian Metrics on Lie Groups

If a smoothly varying, positive definite, bilinear, symmetric form $< .,. >$ is defined on the tangent space at each point on the manifold, such a form is called a Riemannian metric and the manifold is Riemannian [11]. On an $n$-dimensional manifold, the metric is locally characterized by a $n \times n$ matrix of $\mathcal{C}^\infty$ functions $\tilde{g}_{ij} =< X_i, X_j >$, where $X_i$ are basis vector fields. If the basis vector fields can be defined globally, then the matrix $[\tilde{g}_{ij}]$ completely defines the metric.

On $SE(3)$ (on any Lie group), an inner product on the Lie algebra can be extended to a Riemannian metric over the manifold using left (or right) translation. To see this, consider the inner product of two elements $S_1, S_2 \in se(3)$ defined by

$$< S_1, S_2 >_I = s_1^{\mathsf{T}} \tilde{G} s_2, \tag{21.10}$$

where $s_1$ and $s_2$ are the $6 \times 1$ vectors of components of $S_1$ and $S_2$ with respect to some basis, and $G$ is a positive definite matrix. If $V_1$ and $V_2$ are tangent vectors at an arbitrary group element $A \in SE(3)$, the inner product $< V_1, V_2 >_A$ in the tangent space $T_A SE(3)$ can be defined by:

$$< V_1, V_2 >_A = < A^{-1} V_1, A^{-1} V_2 >_I . \tag{21.11}$$

The metric satisfying the above equation is said to be *left invariant* [11]. Right invariance is defined similarly. A metric is *bi-invariant* if it is both left and right invariant.

### 21.2.3 Geodesics and Minimum Acceleration Curves

Any motion of a rigid body is described by a smooth curve $A(t) \in SE(3)$. The velocity is the tangent vector to the curve $V(t) = \frac{\mathrm{d}A}{\mathrm{d}t}(t)$.

An *affine connection* on $SE(3)$ is a map that assigns to each pair of $C^\infty$ vector fields $X$ and $Y$ on $SE(3)$ another $C^\infty$ vector field $\nabla_X Y$, which is bilinear in $X$ and $Y$ and, for any smooth real function $f$ on $SE(3)$ satisfies $\nabla_{fX} Y = f \nabla_X Y$ and $\nabla_X fY = f \nabla_X Y + X(f)Y$.

The *Christoffel symbols* $\Gamma^i_{jk}$ of the connection at a point $A \in SE(3)$ are defined by $\nabla_{\bar{L}_j} \bar{L}_k = \Gamma^i_{jk} \bar{L}_i$, where $\bar{L}_1, \ldots, \bar{L}_6$ is the basis in $T_A SE(3)$ and the summation is understood.

If $A(t)$ is a curve and $X$ is a vector field, the *covariant derivative* of $X$ along $A$ is defined by $\mathrm{D}X/\mathrm{d}t = \nabla_{\dot{A}(t)} X$. Vector field $X$ is said to be *autoparallel* along $A$ if $DX/dt = 0$. A curve $A$ is a *geodesic* if $\dot{A}$ is autoparallel along $A$. An equivalent characterization of a geodesic is the following set of equations:

$$\ddot{a}^i + \Gamma^i_{jk} \dot{a}^j \dot{a}^k = 0, \tag{21.12}$$

where $a_i$, $i = 1, \ldots, 6$ is an arbitrary set of local coordinates on $SE(3)$. Geodesics are also minimum length curves. The length of a curve $A(t)$ between

the points $A(a)$ and $A(b)$ is defined to be $\mathbf{L}(A) = \int_a^b < V, V >^{\frac{1}{2}} \mathrm{d}t$, where $V = \frac{\mathrm{d}A(t)}{\mathrm{d}t}$. It can be shown [11] that if there exists a curve that minimizes the functional $L$, this curve also minimizes the so-called *energy functional*:

$$\mathbf{E}(A) = \int_a^b < V, V > \mathrm{d}t. \tag{21.13}$$

For a manifold with a Riemannian (or pseudo-Riemannian) metric, there exists a unique symmetric connection that is compatible with the metric [11]. Given a connection, the acceleration and higher derivatives of the velocity can be defined. The acceleration $\mathcal{A}(t)$ is the covariant derivative of the velocity along the curve $\mathcal{A} = \frac{\mathrm{D}}{\mathrm{d}t}\left(\frac{\mathrm{d}A}{\mathrm{d}t}\right) = \nabla_V V$. Minimum acceleration curves are defined as curves minimizing the square of the $L^2$ norm of the acceleration:

$$\mathbf{A}(A) = \int_a^b < \nabla_V V, \nabla_V V > \mathrm{d}t, \tag{21.14}$$

where $V(t) = \frac{\mathrm{d}A(t)}{\mathrm{d}t}$, $A(t)$ is a curve on the manifold, and $\nabla$ is the unique symmetric connection compatible with the given metric. The initial and final point as well as the initial and final velocity for the motion are prescribed.

### 21.2.4 The Kinetic Energy Metric

A metric that is attractive for trajectory planning can be obtained by considering the dynamic properties of the rigid body. The kinetic energy of a rigid body is a scalar that does not depend on the choice of the inertial reference frame. It thus defines a left-invariant metric . If the body-fixed reference frame is attached at the centroid the matrix $\tilde{G}$ as in Eq. (21.10)

$$\tilde{G} = \frac{1}{2}\begin{bmatrix} G & 0 \\ 0 & mI \end{bmatrix}, \tag{21.15}$$

where $m$ is the mass of the rigid body, and $G$ is the inertia matrix of the body about the body frame $\{M\}$. If $\{\omega, v\} \in se(3)$ is the vector pair associated with some velocity vector $V$, the norm of the vector $V$ assumes the familiar expression of the kinetic energy:

$$< V, V >= \frac{1}{2}\omega^{\mathrm{T}} G\omega + \frac{1}{2} m v^{\mathrm{T}} v. \tag{21.16}$$

In [36] it was proved that a geodesic $A(t)$ on $SE(3)$ equipped with metric (21.15) is described by

$$\frac{\mathrm{d}\omega}{\mathrm{d}t} = -G^{-1}(\omega \times (G\omega)), \tag{21.17}$$

$$\ddot{d} = 0. \tag{21.18}$$

If $G = \alpha I$, an analytical expression for the geodesic passing through

$$A(0) = (R(0), d(0)),\ A(1) = (R(1), d(1)) \tag{21.19}$$

at $t = 0$ and $t = 1$, respectively, is given by [36]

$$A(t) = (R(t), d(t)) \in SE(3), \tag{21.20}$$

where

$$R(t) = R(0)\exp(\hat{\omega}_0 t), \tag{21.21}$$

$$\hat{\omega}_0 = \log(R(0)^{\mathrm{T}} R(1)), \tag{21.22}$$

and

$$d(t) = (d(1) - d(0))t + d(0) \tag{21.23}$$

In the case when $G \neq \alpha I$, there is no closed-form expression for the corresponding geodesic, and numerical methods should be employed.

If $G = \alpha I$, the differential equations to be satisfied by a minimum acceleration curve are [36]:

$$\omega^{(3)} + \omega \times \ddot{\omega} = 0 \tag{21.24}$$

$$d^{(4)} = 0, \tag{21.25}$$

As observed in [23], Eq. (21.24) can be integrated to obtain $\omega^{(2)} + \omega \times \dot{\omega} =$ constant. However, this equation cannot be further integrated analytically for arbitrary boundary conditions. In [36] it is shown that for special choice of the initial and final velocities, minimum acceleration curves are reparameterized geodesics. If $G \neq \alpha I$ in metric (21.15), the differential equations to be satisfied by the minimum acceleration curves are difficult to derive and are not suited for numerical integration.

## 21.3 An SVD-Based Method for Interpolation on $SE(3)$

In this section it is shown that there is a simple way of defining a left- or right-invariant metric on $SO(n)$ ($SE(n)$) by introducing an appropriate constant metric in $GL^+(n)$ ($GA^+(n)$). Defining a metric (i.e., the kinetic energy) at the Lie algebra $so(n)$ (or $se(n)$) and extending it through left (right) translations is equivalent to inheriting the appropriate metric at each point from the ambient manifold.

### 21.3.1 Riemannian Metrics on $SO(n)$ and $SE(n)$

#### 3.1.1 A Metric in $GL^+(n)$

Let $W$ be a symmetric positive definite $n \times n$ matrix. For any $M \in GL^+(n)$ and any $X, Y \in T_M GL^+(n)$, define

$$< X, Y >_{GL^+} = \mathrm{Tr}(X^{\mathrm{T}} Y W) = \mathrm{Tr}(W X^{\mathrm{T}} Y) = \mathrm{Tr}(Y W X^{\mathrm{T}}). \quad (21.26)$$

By definition, form (21.26) is the same at all points in $GL^+(n)$. It is easy to see that Eq. (21.26) is a Riemmanian metric on $GL^+(n)$ when $W$ is symmetric and positive definite. The following interesting result is proved in [4]:

**Proposition 1.** *The metric given by Eq. (21.26) defined on $GL^+(n)$ is left invariant when restricted to $SO(n)$. The restriction on $SO(n)$ is bi-invariant if $W = \alpha I$, $\alpha > 0$, where $I$ is the $n \times n$ identity matrix.*

*Remark 1.* If right invariance on $SO(n)$ is desired (and left invariance is not needed), we can define

$$<< X, Y >>_{GL^+} = \mathrm{Tr}(X Y^{\mathrm{T}} W) = \mathrm{Tr}(Y^{\mathrm{T}} W X) = \mathrm{Tr}(W X Y^{\mathrm{T}}).$$

Similarly, metric $<<, >>_{GL^+}$ will be right invariant on $SO(n)$ for $W$ symmetric and positive definite and bi-invariant if $W = \alpha I$.

### 3.1.2 The Induced Metric on $SO(3)$

Let $R \in SO(3)$, $X, Y \in T_R SO(3)$, and $R_x(t), R_y(t)$ the corresponding local flows so that

$$X = \dot{R}_x(t),\ Y = \dot{R}_y(t),\ R_x(t) = R_y(t) = R.$$

The metric inherited from $GL^+(3)$ can be written as:

$$< X, Y >_{SO} = < X, Y >_{GL^+} = \mathrm{Tr}(\dot{R}_x^{\mathrm{T}}(t) \dot{R}_y(t) W) =$$

$$= \mathrm{Tr}(\dot{R}_x^{\mathrm{T}}(t) R R^{\mathrm{T}} \dot{R}_y(t) W) = \mathrm{Tr}(\hat{\omega}_x^{\mathrm{T}} \hat{\omega}_y W),$$

where $\hat{\omega}_x = R_x(t)^{\mathrm{T}} \dot{R}_x(t)$ and $\hat{\omega}_y = R_y(t)^{\mathrm{T}} \dot{R}_y(t)$ are the corresponding twists from the Lie algebra $so(3)$. If we write the above relation using the vector form of the twists, some elementary algebra leads to:

$$< X, Y >_{SO} = \omega_x^{\mathrm{T}} G \omega_y, \quad (21.27)$$

where

$$G = \mathrm{Tr}(W) I_3 - W \quad (21.28)$$

is the matrix of the metric on $SO(3)$ as defined by Eq. (21.10). A different but equivalent way of arriving at the expression of $G$ as in Eq. (21.28) would be defining the metric in $so(3)$ i.e., at identity of $SO(3)$) as being the one inherited from $T_I GL^+(3)$: $g_{ij} = \mathrm{Tr}(L_i^{o\mathrm{T}} L_j^o W)$, $i, j = 1, 2, 3$ ($L_1^o, L_2^o, L_3^o$ is the basis in $so(3)$). Left-translating this metric throughout the manifold is equivalent to inheriting the metric at each three-dimensional tangent space of $SO(3)$ from the corresponding nine-dimensional tangent space of $GL^+(3)$.

Using Eq. (21.28), it is easy to verify that the metric $W$ on $GL^+(3)$ and the induced metric $G$ on $SO(3)$ share the following properties:

- $G$ is symmetric if and only if $W$ is symmetric.
- If $W$ is positive definite, then $G$ is positive definite.
- If $G$ is positive definite, then $W$ is positive definite if and only if the eigenvalues of $G$ satisfy the triangle inequality.

In the particular case when $W = \alpha I$, $\alpha > 0$, from Eq. (21.28), we have $G = 2\alpha I$, which is the standard bi-invariant metric on $SO(3)$. This is consistent with the second assertion in Proposition 1. For $\alpha = 1$, metric (21.26) induces the well-known Frobenius matrix norm on $GL^+(3)$ [17].

The quadratic form $\omega^{\mathrm{T}} G \omega$ associated with metric (21.27) can be interpreted as the (rotational) kinetic energy. Consequently, $2G$ can be thought of as the inertia matrix of a rigid body with respect to a certain choice of the body frame $\{M\}$. The triangle inequality restriction on the eigenvalues of $G$ therefore simply states that the principal moments of inertia of a rigid body satisfy the triangle inequality, which, by definition, is true for any rigid body. Therefore, for an arbitrarily shaped rigid body with inertia matrix $2G$, we can formulate a (positive definite) metric (21.26) in the ambient manifold $GL^+(3)$ with matrix

$$W = \frac{1}{2}\mathrm{Tr}(G) I_3 - G. \tag{21.29}$$

Thus Eq. (21.29) gives us a formula for constructing an ambient metric space that is compatible with the given metric structure of $SO(3)$.

### 3.1.3 A Metric in $GA^+(n)$

Let

$$\tilde{W} = \begin{bmatrix} W & a \\ a^{\mathrm{T}} & w \end{bmatrix} \tag{21.30}$$

be a symmetric positive definite $(n+1)\times(n+1)$ matrix, where $W$ is the matrix of metric (21.26), $a \in \mathbb{R}^n$, and $w \in \mathbb{R}$. Let $X$ and $Y$ be two vectors from the tangent space at an arbitrary point of $GA^+(n)$ ($X$ and $Y$ are $(n+1)\times(n+1)$ matrices with all entries of the last row equal to zero). A quadratic form

$$< X, Y >_{GA^+} = \mathrm{Tr}(X^{\mathrm{T}} Y \tilde{W}) \tag{21.31}$$

is symmetric and positive definite if and only if $\tilde{W}$ is symmetric and positive definite.

### 3.1.4 The Induced Metric in $SE(3)$

We can get a left-invariant metric on $SE(n)$ by letting $SE(n)$ inherit the metric $< . >_{GA^+}$ given by Eq. (21.31) from $GA^+(n)$.

Let $A$ be an arbitrary element from $SE(3)$. Let $X, Y$ be two vectors from $T_A SE(3)$, and $A_x(t), A_y(t)$ the corresponding local flows so that

$$X = \dot{A}_x(t),\ Y = \dot{A}_y(t),\ A_x(t) = A_y(t) = A.$$

Let

$$A_i(t) = \begin{bmatrix} R_i(t) & d_i(t) \\ 0 & 1 \end{bmatrix},\ i \in \{x, y\}$$

and the corresponding twists at time $t$:

$$S_i = A_i^{-1}(t)\dot{A}_i(t) = \begin{bmatrix} \hat{\omega}_i & v_i \\ 0 & 0 \end{bmatrix},\ i \in \{x, y\}.$$

The metric inherited from $GA^+(3)$ can be written as:

$$< X, Y >_{SE} = < X, Y >_{GA^+} = \mathrm{Tr}(\dot{A}_x^{\mathrm{T}}(t)\dot{A}_y(t)\tilde{W}) = \mathrm{Tr}(S_x^{\mathrm{T}}A^{\mathrm{T}}AS_y\tilde{W}).$$

Now using the orthogonality of the rotational part of $A$ and the special form of the twist matrices, a straightforward calculation leads to the result:

$$< X, Y >_{SE} = \mathrm{Tr}(S_x^{\mathrm{T}}S_y\tilde{W}) = \mathrm{Tr}(\hat{\omega}_x^{\mathrm{T}}\hat{\omega}_y W) + \mathrm{Tr}(\hat{\omega}_x^{\mathrm{T}}v_y a^{\mathrm{T}}) + v_x^{\mathrm{T}}\hat{\omega}_y a + v_x^{\mathrm{T}}v_y w$$

If $G$ is the matrix of the metric in $SO(3)$ induced by $GL^+(3)$, then

$$< X, Y >_{SE} = \begin{bmatrix} \omega_x^{\mathrm{T}} & v_x^{\mathrm{T}} \end{bmatrix} \tilde{G} \begin{bmatrix} \omega_y \\ v_y \end{bmatrix},\ \tilde{G} = \begin{bmatrix} G & \hat{a} \\ -\hat{a} & wI_3 \end{bmatrix}, \tag{21.32}$$

and $G$ is given by Eq. (21.28).

The metric given by Eq. (21.32) is left invariant since the matrix $\tilde{G}$ of this metric in the left invariant basis vector field is constant. Also, if $\tilde{W}$ is symmetric and positive definite, then $\tilde{G}$ given by Eq. (21.32) is symmetric and positive definite.

The quadratic form $s^{\mathrm{T}}\tilde{G}s$ associated with metric (21.32) can be interpreted as being the kinetic energy of a moving (rotating and translating) rigid body, where $w$ is twice the mass $m$ of the rigid body. If the body fixed frame $\{M\}$ is placed at the centroid of the body, then $a = 0$. Moreover, if $\{M\}$ is aligned with the principal axes of the body, then $G = \frac{1}{2}H$, where $H$ is the diagonal inertia matrix of the body. In the most general case, when the frame $\{M\}$ is displaced by some $(R_0, d_0)$ from the centroid and the orientation parallel with the principal axes, we have [36]:

$$G = R_0^{\mathrm{T}}HR_0 - mR_0^{\mathrm{T}}\hat{d}_0R_0,\ \ a = -mR_0d_0.$$

### 21.3.2 Projection on $SO(n)$

We can use the norm induced by metric (21.26) to define the distance between elements in $GL^+(3)$. Using this distance, for a given $M \in GL^+(3)$, we define *the projection* of $M$ on $SO(3)$ as being the closest $R \in SO(3)$ with respect to the metric from Eq. (21.26). The solution of the projection problem is derived for the general case of $GL^+(n)$ [4]:

**Proposition 2.** *Let $M \in GL^+(n)$ and $U, \Sigma, V$ the singular value decomposition of $MW$ (i.e., $MW = U\Sigma V^{\mathrm{T}}$). Then the projection of $M$ on $SO(n)$ with respect to metric (21.26) is given by $R = UV^{\mathrm{T}}$.*

It is easy to see that the distance between $M$ and $R$ in metric (21.26) is given by $\mathrm{Tr}(W^{-1}V\Sigma^2V^{\mathrm{T}}) + \mathrm{Tr}(W) - 2\mathrm{Tr}(\Sigma)$. For the particular case when $W = I_3$, the distance becomes $\sum_{i=1}^{n}(\sigma_i - 1)^2$, which is the standard way of describing how far a matrix is from being orthogonal.

The question we ask is what happens with the solution to the projection problem when the manifold $GL^+(n)$ is acted upon by the group $SO(n)$. The answer is given below and the proof in [4].

**Proposition 3.** *The solution to the projection problem on $SO(n)$ is left invariant under actions of elements from $SO(n)$. If $W = \alpha I_3$, the solution is bi-invariant.*

For the case $W = I$, it is worthwhile to note that other projection methods do not exhibit bi-invariance. For instance, it is customary to find the projection $R \in SO(n)$ by applying a Gram–Schmidt procedure (QR decomposition). In this case it is easy to see that the solution is left invariant, but in general it is not right invariant.

### 21.3.3 Projection on $SE(n)$

Similar to the previous section, if a metric of the form given in Eq. (21.31) is defined on $GA^+(n)$ with the matrix of the metric given by Eq. (21.30), we can find the corresponding projection on $SE(n)$. We consider the case $a = 0$, which corresponds to a body frame $\{M\}$ fixed at the centroid of the body.

**Proposition 4.** *Let $B \in GA^+(n)$ with the following block partition:*

$$B = \begin{bmatrix} B_1 & B_2 \\ 0 & 1 \end{bmatrix},\ B_1 \in GL^+(n),\ B_2 \in \mathbb{R}^n,$$

*and $U, \Sigma, V$ be the singular value decomposition of $B_1W$. Then the projection of $B$ on $SE(n)$ is given by*

$$A = \begin{bmatrix} UV^{\mathrm{T}} & B_2 \\ 0 & 1 \end{bmatrix} \in SE(n).$$

The proof is given in [4]. Similar to the $SO(n)$ case, the projection on $SE(n)$ exhibits interesting invariance properties.

**Proposition 5.** *The solution to the projection problem on $SE(n)$ is left invariant under actions of elements from $SE(n)$. In the special case when $W = \alpha I$, the projection is bi-invariant under rotations.*

### 21.3.4 The Projection Method

Based on the results we presented so far, we can outline a method to generate an interpolating curve $A(t) \in SE(3)$, $t \in [0, 1]$ while satisfying the boundary conditions:

$$A(0),\, A(1),\, \dot{A}(0),\, \dot{A}(1), \ldots, A^{(m)}(0),\, A^{(m)}(1),$$

where the superscript $(\cdot)^{(m)}$ denotes the $m$th derivative. The projection procedure consists of two steps:

- **Step 1:** Generating the optimal curve $B(t)$ in the ambient manifold $GA^+(3)$ that satisfies the boundary conditions, and
- **Step 2:** Projecting $B(t)$ from step 1 onto $A(t) \in SE(3)$.

Because the metric we defined on $GA^+(3)$ is the same at all points, the corresponding Christoffel symbols are all zero. Consequently, the optimal curves in the ambient manifold assume simple analytical forms. For example, geodesics are straight lines, minimum acceleration curves are cubic polynomial curves, and minimum jerk curves are fifth-order polynomial curves in $GA^+(3)$, all parameterized by time. Therefore, in step 1 the following curve is constructed in $GA^+(3)$:

$$B(t) = B_0 + B_1 t + \ldots + B_{2m-1} t^{2m-1},$$

where the coefficients $B_i$ $i = 1, \ldots, 2m-1$ are linear functions $\Gamma_i$ of the input data:

$$B_i = \Gamma_i \left( A(0), A(1), \dot{A}(0), \dot{A}(1), \ldots, A^{(m)}(0), A^{(m)}(1) \right).$$

Step 2 consists of a singular value decomposition (SVD) decomposition weighted by the matrix $W$ as described in Proposition 4 to produce the curve $A(t)$. Using the linearity of $\Gamma_i$ and Proposition 5, we can prove:

**Proposition 6.** *The projection method on $SE(3)$ is left invariant, i.e., the generated trajectories are independent of the choice of the inertial frame $\{F\}$.*

Because of the linearity on the boundary conditions of the curve in the ambient manifold, the first step is always bi-invariant, i.e., invariant to arbitrary displacements in both the inertial frame $\{F\}$ and the body frame $\{M\}$. The invariance properties of the overall method are, therefore, dictated by the second step. According to Proposition 5, the procedure is bi-invariant with respect only to rotations of $\{F\}$ in the particular case of $W = \alpha I$. In the most general case, i.e., for arbitrary choices of $W$, the method is left invariant to arbitrary displacements of the inertial frame.

### 21.3.5 Geodesics and Minimum Acceleration Curves

Consider a rigid body with inertial properties described by inertia matrix $G$ (in a frame placed at the centroid) and mass $m$. As shown in Sect. 21.2.4, the

kinetic energy of the body can be written in terms of a product metric given in Eq. (21.15). Given two boundary conditions for the pose $A(0) = (R(0), d(0))$ at $t = 0$ and $A(1) = (R(1), d(1))$ at $t = 1$, the translational part of the geodesic interpolant is simply the linear interpolant. The rotational part is constructed by numerically solving a boundary value problem consisting of end values $R(0)$ and $R(1)$ and the system of differential equations (21.17) augmented by the expressions of the time derivatives of some chosen coordinates on $SO(3)$ (exponential coordinates, Euler angles, quaternions) [3]. The relaxation or the shooting method are among the most popular [26]. For $G = \alpha I$, the interpolating minimum acceleration curve for the same position end conditions and velocity boundary conditions $\dot{R}(0)$, $\dot{d}(0)$, $\dot{R}(1)$, $\dot{d}(1)$ has a cubic translational part. The interpolating rotation can be found by solving a boundary value problem consisting of $R(0)$, $\dot{R}(0)$, $R(1)$, $\dot{R}(1)$ and 12 differential equations: Eq. (21.24) and the derivatives of the parameterization.

If the projection method described above is used, an approximate geodesic for the metric given in Eq. (21.15) and the same boundary conditions is given by

$$d(t) = d(0) + (d(1) - d(0))t, \quad R(t) = U(t)V^{\mathrm{T}}(t),$$

with $U$ and $V$ determined from the weighted SVD

$$M(t)W = U(t)\Sigma(t)V^{\mathrm{T}}(t),$$

where

$$M(t) = R(0) + (R(1) - R(0))t, \; W = \frac{1}{2}\mathrm{Tr}(G)I_3 - G.$$

Similarly, an approximate minimum acceleration curve can be constructed as

$$d(t) = d_0 + d_1 t + d_2 t^2 + d_3 t^3, \quad R(t) = U(t)V^{\mathrm{T}}(t),$$

where

$$d_0 = d(0), \; d_1 = \dot{d}(0), \; d_2 = -3d(0) + 3d(1) - 2\dot{d}(0) - \dot{d}(1),$$

$$d_3 = 2d(0) - 2d(1) + \dot{d}(0) + \dot{d}(1),$$

$$M(t) = M_0 + M_1 t + M_2 t^2 + M_3 t^3,$$

$$M_0 = R(0), \; M_1 = \dot{R}(0), \; M_2 = -3R(0) + 3R(1) - 2\dot{R}(0) - \dot{R}(1),$$

$$M_3 = 2R(0) - 2R(1) + \dot{R}(0) + \dot{R}(1)$$

For geodesics on $SO(3)$ with Euclidean metric, we prove [4] that the projection of the geodesic from $GL^+(3)$ and the true geodesic on $SO(3)$ follow the same path but with different parameterizations. However, one can reparameterize the geodesic from $GL^+(3)$ so that it projects to the exact geodesic on $SO(3)$. We also show that uniqueness of projected geodesics and minimum acceleration curves is guaranteed under reasonable assumptions on the amount of rotation and the magnitude of the end velocities. In [3], we show

that, from a computational point of view, it is much less expensive to generate interpolating motion using the projection method as opposed to the relaxation method. Specifically, if $M$ is the number of uniformly distributed time points in [0, 1], then the number of flops required by the projection method in $GL^+(n)$ is of order $O(n^3M)$. On the other hand, the number of flops required by the relaxation method for generating solution at $M$ mesh points of a system of $N$ differential equations with boundary conditions is of order $O(M^3N^3)$. For example, generating geodesics on $SO(3)$ at $M = 100$ time points involves millions of flops by the relaxation method, while only thousands by the projection method.

### 21.3.6 Simulation Results

In this section, we generate motion for a homogeneous parallelepipedic rigid body We assume that the body frame $\{M\}$ is placed at the center of mass and aligned with the principal axes of the body. Let $a$, $b$, and $c$ be the lengths of the body along its $x$, $y$, and $z$ axes respectively, and $m$ the mass of the body. For visualization, a small square is drawn on one of its faces and the center of the parallelepiped is shown starred.

The matrix $G$ of metric $<,>_{SO}$ is given by

$$G = \begin{bmatrix} \frac{m}{24}(b^2+c^2) & 0 & 0 \\ 0 & \frac{m}{24}(a^2+c^2) & 0 \\ 0 & 0 & \frac{m}{24}(a^2+b^2) \end{bmatrix}. \tag{21.33}$$

True and projected minimum acceleration motions for a cubic rigid body with $a = b = c = 2$ and $m = 12$ are given in Fig. 21.2 for comparison. Note that for this case $G = \alpha I$ with $\alpha = 4$. Geodesics for the same boundary conditions and a parallelepipedic body with $a = c = 2$, $b = 10$ and $m = 12$ are given in Fig. 21.3.

As seen in Figs. 21.2 and 21.3, even though the total displacement between the initial and final positions on $SO(3)$ is large (rotation angle of $\pi\sqrt{14}/6$), there is no noticeable difference between the true and the projected motions.

## 21.4 Optimal Motion Generation for Groups of Robots

This section presents a method for generating smooth trajectories for a set of mobile robots satisfying constraints on relative positions. It is shown that, given two end configurations of the set of robots, by tuning one parameter, the user can choose an interpolating trajectory from a continuum of curves varying from the trajectory corresponding to maintaining a rigid formation to trajectories that allow the formation to change and the robots to reconfigure while moving.

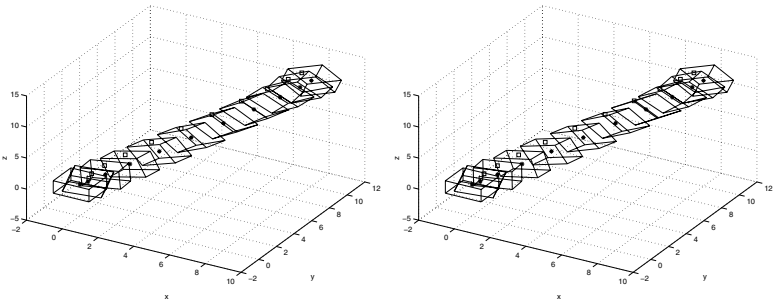

(a) (b)

**Fig. 21.2. a,b**. Minimum acceleration motion for a cube in free space: **a** relaxation method, **b** projection method

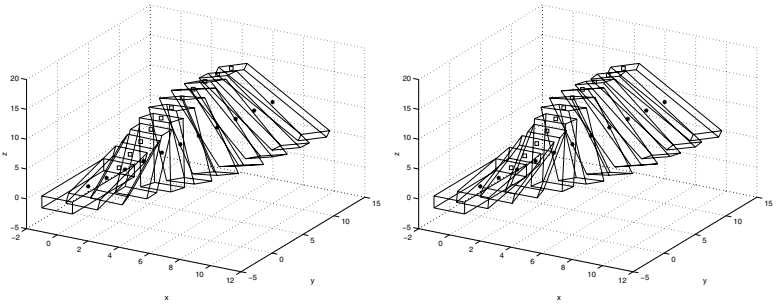

(a) (b)

**Fig. 21.3. a,b**. Geodesics for a parallelepipedic body: **a** relaxation method, **b** projection method

### 21.4.1 Problem Statement and Notation

Consider $N$ robots moving (rotating and translating) in 3D space with respect to an inertial frame $\{F\}$. We choose a reference point on each robot at its center of mass $O_i$. A moving frame $\{M_i\}$ is attached to each robot at $O_i$ (see Fig. 21.4).

Robot $i$ has mass $m_i$ and matrix of inertia $H_i$ with respect to frame $\{M_i\}$. Let $R_i \in SO(3)$ denote the rotation of $\{M_i\}$ in $\{F\}$ and $q_i \in \mathbb{R}^3$ the position vector of $O_i$ in $\{F\}$. Let $\omega_i$ denote the expression in $\{M_i\}$ of the angular velocity of $\{M_i\}$ with respect to $\{F\}$. The *formation* is defined by the reference points $O_i$. The moving formation is called *rigid* if the relative distance between any of the points $O_i$ is maintained constant. Sometimes it is also useful to define a *formation frame* $\{M\}$, attached at some virtual point $O'$ and with pose $(R, d) \in SE(3)$ in $\{F\}$. Let $q_i^0$ denote the position vectors of $O_i$ in $\{M\}$.

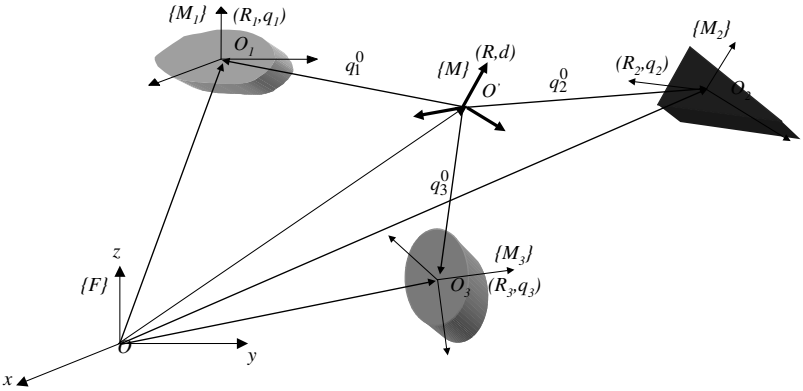


**Fig. 21.4.** A set of $N = 3$ robots

The configuration space is the $6N$-dimensional manifold, $SE(3)\times, \ldots, \times SE(3)$, given by the poses of each robot. Given two configurations at times $t = 0$ and $t = 1$ respectively, the goal is to generate smooth interpolating motion for each robot so that the total kinetic energy is minimized.

The kinetic energy $T$ of the system of robots is the sum of the individual energies. Since the frames $\{M_i\}$ were placed at the centroids $O_i$ of the robots, $T$ can be written as the sum of the total rotational energy $T_r$ and the total translational energy $T_t$ in the form:

$$T = T_r + T_t, \;\; T_r = \frac{1}{2}\sum_{i=1}^{N}(\omega_i^{\mathrm{T}} H_i \omega_i), \; T_t = \frac{1}{2}\sum_{i=1}^{N}(m_i \dot{q}_i^{\mathrm{T}} \dot{q}_i). \tag{21.34}$$

Since our definition of a formation only involves the reference points $O_i$, a formation requirement will only constrain the $q_i$'s from the above equation. Therefore, as a result of the decomposition in Eq. (21.34), minimizing the total energy is equivalent to solving $N + 1$ independent optimization subproblems:

$$\min_{\sigma_i} \int_0^1 \omega_i^{\mathrm{T}} H_i \omega_i \mathrm{d}t, \; i = 1, \ldots, N, \tag{21.35}$$

$$\min_{q_i = 1, \ldots, N} \int_0^1 T_t \mathrm{d}t \tag{21.36}$$

where $\sigma_i$ is some parameterization of the rotation of $\{M_i\}$ in $\{F\}$, i.e., some local coordinates on $SO(3)$. The solutions to Eq. (21.35) are given by $N$ geodesics on $SO(3)$ with left-invariant metrics with matrices $H_i$. A relaxation method [26] or the projection method described in Section 21.3 can be used to generate the solution. An example is given in Sect. 21.4.4.

The main focus in this section is solving the problem given by Eq. (21.36) while satisfying constraints on the positions of the reference points $O_i$ that

may be imposed by the requirements on the task. Thus the configuration space we are interested in is just the $3N$-dimensional $Q = \{q | q = (q_1, \ldots, q_N)\}$ that collects all the position vectors of the chosen reference points. Maintaining a rigid formation (a virtual structure) imposes constraints on the configuration space, $Q$, and these constraints may be relaxed as necessary.

### 21.4.2 The Rigidity Constraint: Virtual Structures

The group of $N$ robots is said to form a *virtual structure* if the relative distance between any of the reference points $O_i$ is maintained constant. Let $q = [q_1^{\mathrm{T}}, \ldots, q_N^{\mathrm{T}}]^{\mathrm{T}}$ denote an arbitrary point in $Q$. For an arbitrary pair of reference points with position vectors $q_i$ and $q_j$, $i, j = 1, \ldots, N$, $i < j$, the constraints can be written as:

$$(q_i - q_j)^{\mathrm{T}}(q_i - q_j) = constant, \tag{21.37}$$

or, by differentiation:

$$(q_i - q_j)^{\mathrm{T}}\dot{q}_i - (q_i - q_j)^{\mathrm{T}}\dot{q}_j = 0.$$

By lifting this constraint to the configuration manifold $Q$, the coordinates of the corresponding differential one form can be written as a $1 \times 3N$ row vector:

$$\omega_{ij} = \left[ 0 \ldots 0 \ (q_i - q_j)^{\mathrm{T}} \ 0 \ldots 0 \ -(q_i - q_j)^{\mathrm{T}} \ 0 \ldots 0 \right].$$

The nonzero $1 \times 3$ blocks in the above matrix are in positions $i$ and $j$, respectively. If we consider all $(N-1)N/2$ possible constraints, we can construct the codistribution $\omega_R$ as the span of all the corresponding covectors:

$$\omega_R = \mathrm{span}\left\{\omega_{ij},\, i, j = 1, \ldots, N,\, i < n\right\}.$$

It is obvious that not all the $(N-1)N/2$ covectors (constraints) are independent. To insure rigidity, it is necessary and sufficient to impose $2N-3$ constraints of the type (21.37) in plane, while in 3D the number is $3N-6$. By simple inspection, it is easy to prove that the annihilating distribution of $\omega_R$ ($\omega_R(\Delta_R) = 0$) is:

$$\Delta_R = \mathrm{Range}(A(q)),\ A(q) = \begin{bmatrix} -\hat{q}_1 & I_3 \\ \ldots & \ldots \\ -\hat{q}_N & I_3 \end{bmatrix}. \tag{21.38}$$

Therefore, by lifting each constraint to the configuration manifold $Q$, the virtual structure (rigidity) constraint can be written as

$$\dot{q} \in \Delta_R(q). \tag{21.39}$$

If $q_i$ are not all contained in any proper hyperplane of $\mathbb{R}^d$ ($d = 2, 3$), it can be proved [27] that the distribution $\Delta_R$ is regular, and, therefore integrable,

since involutivity is always guaranteed. The distribution $\Delta_R(q)$ determines a foliation of $Q$ with leaves given by orbits of $SE(3)$. Indeed, assume $q(0) = q^0$ and $\dot{q}(0) \in \Delta_R(q^0)$. Then, the rigidity constraint in Eq. (21.39) is satisfied for all $t \geq 0$ if and only if

$$q_i(t) = d(t) + R(t)q_i^0,\ i = 1, \ldots, N, \tag{21.40}$$

where $(R(t), d(t))$ is a trajectory of the left-invariant control system

$$\dot{g}(t) = gS \tag{21.41}$$

starting from $R(0) = I_3$, $d(0) = 0$.

Note that, under the rigidity assumption in Eq. (21.39), the coordinates $r$ of the expansion of $\dot{q} \in \Delta_R(q)$ along the columns of $A(q)$, i.e., $\dot{q} = A(q)r$, are exactly the components of the left-invariant twist of a virtual structure formed by $(q_1, \ldots, q_N)$ and $\{F\}$ at that instant.

Also, if Eq. (21.39) is satisfied, then $s$ from Eq. (21.41) is the left-invariant twist of a moving rigid structure formed by $(q_1^0, \ldots, q_N^0)$ and $\{M\}$ and for which the mobile frame $\{M\}$ was coincident with $\{F\}$ at $t = 0$. The pose of the moving frame $\{M\}$ in $\{F\}$ is $g = (R, d)$. Moreover, we have

$$\dot{q}_i = R[-\hat{q}_i^0\ I]s. \tag{21.42}$$

It follows that motion planning (control) problems for a set of $N$ robots in 3D required to maintain a rigid formation can be reduced to motion planning (control) problems for a left-invariant control system on $SE(3)$.

### 21.4.3 Motion Decomposition: Rigid vs. Nonrigid

We first define a metric $<,>$ in the position configuration space, which is the same at all points $q \in Q$:

$$< V_q^1, V_q^2 >= {V_q^1}^{\mathrm{T}} M V_q^2, \tag{21.43}$$

$$V_q = \dot{q} \in T_qQ,\ \ M = \frac{1}{2}\mathrm{diag}\{m_1 I_3, \ldots, m_N I_3\}.$$

Metric (21.43) is called the *kinetic energy metric* because its induced norm ($V_q^1 = V_q^2 = \dot{q}$) assumes the familiar expression of the kinetic energy of the system $1/2 \sum_{i=1}^{N} m_i \dot{q}_i^{\mathrm{T}} \dot{q}_i$. If no restrictions are imposed on $Q$, the geodesic between $q(0) = q^0$ and $q(1) = q^1$ for metric (21.43) is obviously a straight line uniformly parameterized in time interpolating between $q^0$ and $q^1$ in $Q$.

At each point $q$ in the configuration space $Q$, $\Delta_R(q)$ locally describes the set of all rigid body motion directions. The orthogonal complement to $\Delta_R(q)$, $\Delta_{NR}(q)$, will be the set of all directions violating the rigid body constraints. [3]

[3] In [6], the tangent space at $q$ to the orbit of $SE(3)$ is called the vertical space at $q$, $\mathrm{Ver}_q$, and its orthogonal complement is the horizontal space at $q \in Q$, $\mathrm{Hor}_q$.

For an arbitrary tangent vector $V_q \in T_qQ$, let $\mathbf{R}V_q$ denote the projection onto $\Delta_R$ and $\mathbf{NR}V_q$ denote the projection onto $\Delta_{NR}$.

Using the metric in Eq. (21.43), the orthogonal complement of the "rigid" distribution $\Delta_R(q)$ is the "nonrigid" distribution

$$\Delta_{NR}(q) = \text{Null}(A(q)^{\mathrm{T}} M). \tag{21.44}$$

Let $B(q)$ denote a matrix whose columns are a basis of $\Delta_{NR}(q)$.

Let $\psi$ denote the components of the projection in this basis: $\mathbf{NR}V_q = B(q)\psi$. Therefore, the velocity at point $q$ can be written as:

$$V_q = \mathbf{R}V_q + \mathbf{NR}V_q = A(q)r + B(q)\psi. \tag{21.45}$$

Then, for any $V_q^1$, $V_q^2 \in T_qQ$, we have:

$$< V_q^1, V_q^2 >= {V_q^1}^{\mathrm{T}} M V_q^2 =< \mathbf{NR}V_q^1, \mathbf{NR}V_q^2 > + < \mathbf{R}V_q^1, \mathbf{R}V_q^2 >$$

because both $A^{\mathrm{T}}MB$ and $B^{\mathrm{T}}MA$ are zero from Eq. (21.44). Also, note that

$$r = (A^{\mathrm{T}}MA)^{-1}A^{\mathrm{T}}MV,\ \psi = (B^{\mathrm{T}}MB)^{-1}B^{\mathrm{T}}MV, \tag{21.46}$$

where the explicit dependence of $A$ and $B$ on $q$ was omitted for simplicity. Therefore, the translational kinetic energy (which is the square of the norm induced by metric (21.43)) becomes:

$$T_t(q, \dot{q}) = \dot{q}^{\mathrm{T}} M \dot{q} = r^{\mathrm{T}} A^{\mathrm{T}} MAr + \psi^{\mathrm{T}} B^{\mathrm{T}} MB\psi. \tag{21.47}$$

In (21.47), $r^{\mathrm{T}}A^{\mathrm{T}}MAr$ captures the energy of the motion of the system of particles as a rigid body, while the remaining part $\psi^{\mathrm{T}}B^{\mathrm{T}}MB\psi$ is the energy of the motion that violates the rigid body restrictions. For example, in the obvious case of a system of $N = 2$ particles, the first part corresponds to the motion of the two particles connected by a rigid massless rod, while the second part would correspond to motion along the line connecting the two bodies.

### 21.4.4 Motion Generation for Rigid Formations

In this section, we will assume that the robots are required to move in *rigid formation*, i.e., the distances between any two reference points $O_i$ are preserved, or, equivalently, the reference points form a rigid polyhedron.

In our geometric framework, the rigid body requirement means restricting the trajectory $q(t) \in Q$ to be a $SE(3)$-orbit, or equivalently, $\mathbf{NR}\dot{q} = 0$ or $\dot{q} \in \Delta_R(q)$, for all $q$.

In this case, one can imagine a body frame $\{M\}$ moving with the virtual structure determined by the $O_i$'s. Initially ($t = 0$), the frame $\{M\}$ is coincident with $\{F\}$ and $q(0) = q^0$. The position vector of $O_i$ in $\{M\}$ is constant during this motion and equal to $q_i^0$.

Using Eq. (21.42), the kinetic energy $T_t$ becomes:

$$T_t = s^{\mathrm{T}}\mathcal{M}s, \quad \mathcal{M} = A(q^0)^{\mathrm{T}} M A(q^0), \tag{21.48}$$

where $s \in se(3)$ is the instantaneous twist of the virtual structure.

Therefore, if the set of robots is required to move while maintaining a constant shape $q^0$, the optimization problem is reduced from dimension $6N$ to dimension $3N + 6$, and consists of solving for $N$ geodesics on $SO(3)$ with metrics $H_i$ (individual rotations) and one geodesic on the $SE(3)$ of the virtual structure with left invariant metric $\mathcal{M}$ as in Eq. (21.48).

### 4.4.1 Example: Five Identical Robots in 3D Space

For illustration, we consider five identical parallelepipedic robots with dimensions $a, b, c$ and masses $m_i = m$, $i = 1, \ldots, 5$ required to move in formation while minimizing energy. The virtual structure is a pyramid with a square base of side $l$ and height $h$. The body frames and the formation frame are placed at the center of mass and aligned with the principal axis. As outlined in the previous section, generating optimal motion for this group of robots reduces to generating five geodesics on the $SO(3)$ of each robot with left-invariant metric $H_i = G$ as in Eq. (21.33), $i = 1, \ldots, 5$ and one geodesic on the $SE(3)$ of the virtual structure endowed with a left-invariant metric with matrix

$$\tilde{G} = \frac{m}{2} \begin{bmatrix} 2l^2 & 0 & 0 & 0 \\ 0 & l^2 + \frac{4h^2}{3} & 0 & 0 \\ 0 & 0 & l^2 + \frac{4h^2}{3} & 0 \\ 0 & 0 & 0 & 3I_3 \end{bmatrix}$$

The resulting motion is presented in Fig. 21.5 for numerical values $a = c = 2$, $b = 10$, $m = 12$, $h = 20$, and $l = 10$. The projection method presented in Sect. 21.3 was used to generate the interpolating motions.

### 21.4.5 Motion Generation by Kinetic Energy Shaping

By shaping the kinetic energy , we mean smoothly changing the corresponding metric (21.43) at $T_qQ$ so that motion along some specific directions is allowed while motion along some other directions is penalized. The new metric will no longer be constant: the Christoffel symbols of the corresponding symmetric connection will be nonzero. The associated geodesic flow gives optimal motion.

In this work, the original metric (21.43) is shaped by putting different weights on the terms corresponding to the rigid and nonrigid motions:

$$< V_q^1, V_q^2 >_\alpha = \alpha < \mathbf{N}\mathbf{R}V_q^1, \mathbf{N}\mathbf{R}V_q^2 > + (1-\alpha) < \mathbf{R}V_q^1, \mathbf{R}V_q^2 > . \tag{21.49}$$

Using Eq. (21.46) to go back to the original coordinates, we get the modified metric in the form:

$$< V_q^1, V_q^2 >_\alpha = {V_q^1}^{\mathrm{T}} M_\alpha(q) V_q^2, \tag{21.50}$$

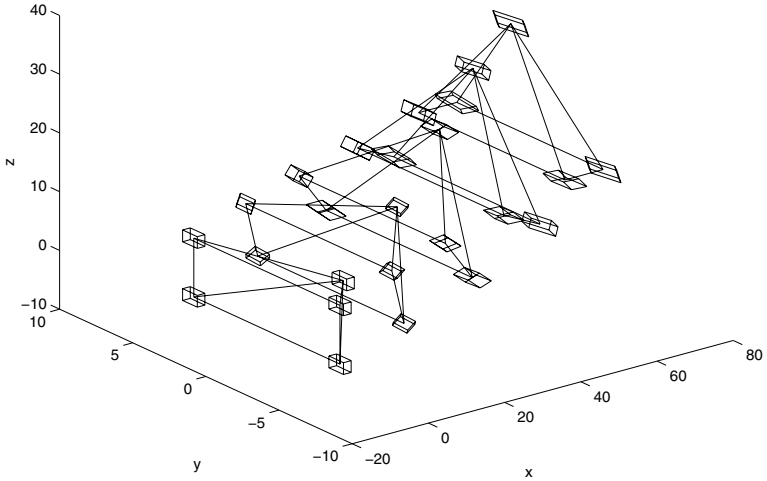


**Fig. 21.5.** Optimal motion for five identical robots required to maintain a rigid formation

where the new matrix of the metric is now dependent on the artificially introduced parameter $\alpha$ and the point on the manifold $q \in Q$:

$$M_\alpha(q) = \alpha MA(A^{\mathrm{T}}MA)^{-\mathrm{T}}A^{\mathrm{T}}M + (1-\alpha)MB(B^{\mathrm{T}}MB)^{-\mathrm{T}}B^{\mathrm{T}}M. \qquad (21.51)$$

The influence of the parameter $\alpha$ can be best seen by examining the significance of $\alpha$ taking on the values of 0, 0.5, and 1. As $\alpha$ tends to 0, the preferred motions will be ones where robots cluster together through much of the duration of the trajectory, thus minimizing the *rigid body energy* consumption. As $\alpha$ approaches 0.5, the motions degenerate toward uncoordinated, independent motions. As $\alpha$ tends to 1, the preferred motions are ones where the robots stay in rigid formation through most of the trajectory, thus minimizing the energy associated with *deforming* the formation.

We use the geodesic flow of metric (21.50) to produce smooth interpolating motion between two given configurations:

$$q^0 = q(0), \;\; q^1 = q(1) \;\in \mathbb{R}^{3N}. \qquad (21.52)$$

To simplify the notation, let $x_i$, $i = 1, \ldots, 3N$ denote the coordinates $q_i \in \mathbb{R}^3$, $i = 1, \ldots, N$ on the configuration manifold $Q$. In this coordinates, the geodesic flow is described by the following differential equations [11]:

$$\ddot{x}_i + \sum_{j,k} \Gamma^i_{jk} \dot{x}_j \dot{x}_k = 0, \; i = 1, \ldots, 3N, \qquad (21.53)$$

where $\Gamma^k_{ij}$ are the Christoffel symbols of the unique symmetric connection associated to metric (21.50):

$$\Gamma_{ij}^{k} = \frac{1}{2}\sum_{h}\left(\frac{\partial m_{hj}}{\partial x^{i}} + \frac{\partial m_{ih}}{\partial x^{j}} - \frac{\partial m_{ij}}{\partial x^{h}}\right) m^{hk}, \tag{21.54}$$

for $m_{ij}$ and $m^{ij}$ elements of $M_\alpha$ and $M_\alpha^{-1}$, respectively.

Because $\alpha = 0$ and $\alpha = 1$ make the metric singular, Eq. (21.54) can only be used for $0 < \alpha < 1$.

### 4.5.1 Example: Two Bodies in Plane

Consider two bodies of masses $m_1$ and $m_2$ moving in the $x$-$y$ plane. The configuration space is $Q = R^4$ with coordinates $q = [x_1, y_1, x_2, y_2]^{\mathrm{T}}$. The $A$ and $B$ matrices describing $\Delta_R(q)$ and $\Delta_{NR}(q)$ as in Eqns. (21.38) and (21.44) are:

$$A = \begin{bmatrix} -y_1 & 1 & 0 \\ x_1 & 0 & 1 \\ -y_2 & 1 & 0 \\ x_2 & 0 & 1 \end{bmatrix}, \quad B = \begin{bmatrix} \frac{m_2(x_2-x_1)}{m_1(y_1-y_2)} \\ -\frac{m_2}{m_1} \\ \frac{x_1-x_2}{y_1-y_2} \\ 1 \end{bmatrix}.$$

The 64 Christoffel symbols $\Gamma^k = (\Gamma_{ij}^k)_{ij}$ of the connection associated with the modified metric at $q \in Q$ become:

$$\Gamma^1 = \frac{2(1-2\alpha)}{\alpha}\frac{m_2}{m_1+m_2}\frac{d_x}{(d_x^2+d_y^2)^2}\Gamma,$$

$$\Gamma^2 = \frac{2(1-2\alpha)}{\alpha}\frac{m_2}{m_1+m_2}\frac{d_y}{(d_x^2+d_y^2)^2}\Gamma,$$

$$\Gamma^3 = -\frac{2(1-2\alpha)}{\alpha}\frac{m_1}{m_1+m_2}\frac{d_x}{(d_x^2+d_y^2)^2}\Gamma,$$

$$\Gamma^4 = -\frac{2(1-2\alpha)}{\alpha}\frac{m_1}{m_1+m_2}\frac{d_y}{(d_x^2+d_y^2)^2}\Gamma,$$

where

$$\Gamma = \begin{bmatrix} -d_y^2 & d_x d_y & d_y^2 & -d_x d_y \\ d_x d_y & -d_x^2 & -d_x d_y & d_x^2 \\ d_y^2 & -d_x d_y & -d_y^2 & d_x d_y \\ -d_x d_y & d_x^2 & d_x d_y & -d_x^2 \end{bmatrix},$$

and $d_x = x_1 - x_2$, $dy = y_1 - y_2$. It can be easily seen that, as expected, all Christoffel symbols are zero if $\alpha = 0.5$. Also, the actual masses of the robots are not relevant, only the ratio $m_1/m_2$ is important.

In this example, we assume $m_2 = 2m_1$ and the boundary conditions:

$$q^0 = \begin{bmatrix} 1 \\ 0 \\ -0.5 \\ 0 \end{bmatrix}, \quad q^1 = \begin{bmatrix} 3 - \frac{\sqrt{2}}{2} \\ -\frac{\sqrt{2}}{2} \\ 3 + \frac{\sqrt{2}}{4} \\ \frac{\sqrt{2}}{4} \end{bmatrix},$$

which correspond to a rigid body displacement so that we can compare our results to the optimal motion corresponding to a rigid body.

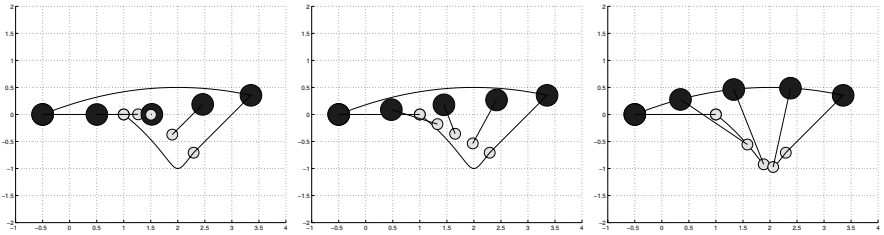


**Fig. 21.6.** Three interpolating motions for a set of two planar robots as geodesics of a modified metric defined in the configuration space

If the structure was assumed rigid, then the optimal motion is described by uniform rectilinear translation of the center of mass between $(0, 0)$ and $(3, 0)$ and uniform rotation between 0 and $3\pi/4$ around $-z$ placed at the center of mass. The corresponding trajectories of the robots are drawn in solid line in all the pictures in Fig. 21.6. It can be easily seen that there is no difference between the optimal motion of the virtual structure solved on $SE(2)$ and the geodesic flow of the modified metric with $\alpha = 0.99$ (Fig. 21.6, right). If $\alpha = 0.5$, all bodies move in straight line as expected (Fig. 21.6, middle). For $\alpha = 0.2$, the bodies go toward each other first, and then split apart to attain the final positions (Fig. 21.6, left).

### 4.5.2 Example: Three Bodies in Plane

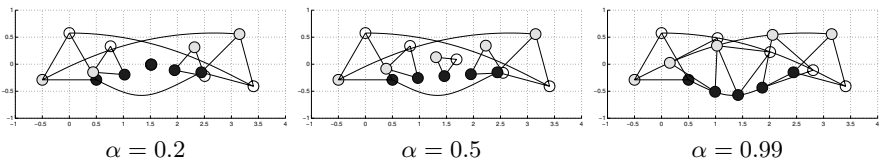


**Fig. 21.7.** Three interpolating motions for a set of three planar robots as geodesics of a modified metric defined in the configuration space

The calculation of the trajectories for three bodies moving in the plane is simplified by assuming that the robots are identical, and, without loss of generality, we assume $m_1 = m_2 = m_3 = 1$. The rigid and the nonrigid spaces at a generic configuration

$$q = [x_1,\, y_1,\, x_2,\, y_2,\, x_3,\, y_3]^{\mathrm{T}} \in Q = \mathbb{R}^6$$

are given by

$$\Delta_R = \mathrm{Range}(A),\ A = \begin{bmatrix} -y_1 & 1 & 0 \\ x_1 & 0 & 1 \\ -y_2 & 1 & 0 \\ x_2 & 0 & 1 \\ -y_3 & 1 & 0 \\ x_3 & 0 & 1 \end{bmatrix},$$

$$\Delta_{NR} = \mathrm{Range}(B),\ B = \begin{bmatrix} \frac{x_3 - x_1}{y_1 - y_2} & \frac{y_2 - y_3}{y_1 - y_2} & \frac{x_2 - x_1}{y_1 - y_2} \\ -1 & 0 & -1 \\ \frac{x_1 - x_3}{y_1 - y_2} & \frac{y_3 - y_1}{y_1 - y_2} & \frac{x_1 - x_2}{y_1 - y_2} \\ 0 & 0 & 1 \\ 0 & 1 & 0 \\ 1 & 0 & 0 \end{bmatrix}.$$

For simplicity, we omit the expressions of the modified metric and of the Christoffel symbols. The simulation scenario resembles the one in Sect. 21.4.5: the end poses correspond to a rigid structure consisting of an equilateral triangle with sides equal to 1. The optimal trajectory solved on $SE(2)$ corresponds to rectilinear uniform motion of the center of mass (line between (0,0) and (3,0) in Fig. 21.7) and uniform rotation from angle 0 to $3\pi/4$ around axis $-z$. The resulting motion of each robot is shown solid, while the actual trajectory for the corresponding value of $\alpha$ is shown dashed. First note for $\alpha = 0.99$ the trajectories are basically identical with the optimal traces produced by the virtual structure, as expected. In the case $\alpha = 0.5$ the bodies move in straight line (corresponding to the unmodified metric). The tendency to cluster as $\alpha$ decreases is seen for $\alpha = 0.2$. Note also that because of our choice $m_1 = m_2 = m_3$, the geometry of the equilateral triangle is preserved for all values of $\alpha$, it only scales down when $\alpha$ decreases from 1.

## 21.5 Conclusion

In this chapter, we survey the problem of generating interpolating motion for groups of robots required to maintain a rigid formation, or virtual structure. Since energy consumption is an important issue, especially for deep space formations, motion planning for virtual structures is often accomplished by posing the problem as an optimization problem. For example, satellite formation reconfiguration demands a fuel-optimal trajectory to preserve mission life and is constrained by the limited thrust available. Also, it is desired that the generated trajectories be independent of a chosen reference frame.

Virtual structures, as rigid bodies, evolve on the Lie group of all translations and orientations in 3D, $SE(3)$. The first part of this chapter is concerned

with optimally interpolating trajectories on $SE(3)$. The second part investigates the rigidity constraint for a team of robots and shows how individual motion plans can be constructed so that the overall energy of the formation is minimized. The methodology and results are organized around two main issues: optimality and invariance of the generated trajectories. The price one has to pay to achieve these is, of course, a large amount of computation. We expect that these methods will only find applications in areas where the number of agents is small and fuel consumption is critical, as in satellite reconfiguration.

When a large number of agents is required to be coordinated and controlled, some level of abstraction is necessary, dependent on the imposed task. The virtual structure approach, which can be seen as an abstraction, is not appropriate in many applications, including passing of a tunnel and obstacle avoidance. Preliminary results on developing a general control method for large groups of inexpensive agents based on abstractions are presented in [5].

## References

1. T. Balch, R. Arkin (1998) Behavior-based formation control for multi-robotic teams. *IEEE Transactions on Robotics and Automation* 14:926–934
2. R. W. Beard, F. Y. Hadaegh (1998) Constellation templates: an approach to autonomous formation flying. In: *World Automation Congress*, pp. 177.1–177.6, Anchorage, Alaska
3. C. Belta, V. Kumar (2002) Euclidean metrics for motion generation on $SE(3)$. *Journal of Mechanical Engineering Science Part C* 216:47–61
4. C. Belta, V. Kumar (2002) An SVD-based projection method for interpolation on se(3). *IEEE Trans. on Robotics and Automation*, 18:334–345
5. C. Belta, V. Kumar (2002). Towards abstraction and control for large groups of robots. In: *Control Problems in Robotics*, *Springer, Berlin Heidelberg New York*, pp. 169–182
6. A.M. Bloch, N.E. Leonard, J.E. Marsden (2000). Controlled lagrangians and the stabilization of mechanical systems 1: the first matching theorem. *IEEE Transactions on Automatic Control*, 45:2253–2270
7. W. Burgard, M. Moors, D. Fox, R. Simmons, S. Thrun (2000) Collaborative multi-robot exploration. In: *Proc. IEEE Int. Conf. Robot. Automat.*, pp. 476–481, San Francisco, CA
8. M. Camarinha, F. Silva Leite, P. Crouch (1995) Splines of class $C^k$ on non-Euclidean spaces. *IMA J. Math. Control Inform.*, 12:399–410
9. P. Crouch, F. Silva Leite (1995) The dynamic interpolation problem: on Riemannian manifolds, Lie groups, and symmetric spaces. *J. Dynam. Control Systems*, 1:177–202
10. J. Desai, J. P. Ostrowski, V. Kumar (1998) Controlling formations of multiple mobile robots. In: *Proc. IEEE Int. Conf. Robot. Automat.*, pp. 2864–2869, Leuven, Belgium
11. M. P. do Carmo (1992) *Riemannian geometry.* Birkhauser, Boston
12. M. Egerstedt, X. Hu (2001) Formation constrained multi-agent control. *IEEE Trans. Robotics and Automation*, 17:947–951

13. T. Eren, P. N. Belhumeur, B. D. O. Anderson, A. S. Morse (2002) A framework for maintaining formations based on rigidity. In: *IFAC World Congress*, pp. 2752–2757, Barcelona, Spain
14. G. E. Farin (1992) *Curves and surfaces for computer aided geometric design : a practical guide, 3rd edn*, Academic Press, Boston
15. J. Feddema, D. Schoenwald (2001) Decentralized control of cooperative robotic vehicles. In: *Proc. SPIE Vol. 4364, Aerosense*, Orlando, Florida
16. Q. J. Ge, B. Ravani (1994) Computer aided geometric design of motion interpolants. *ASME Journal of Mechanical Design*, 116:756–762
17. G. H. Golub, C. F. van Loan (1989) *Matrix computations*. The Johns Hopkins University Press, Baltimore
18. B. Juttler, M. Wagner (1996) Computer aided design with rational b-spline motions. *ASME J. of Mechanical Design*, 118:193–201
19. N. E. Leonard, E. Fiorelli (2001) Virtual leaders, artificial potentials, and coordinated control of groups. In: *40th IEEE Conference on Decision and Control*, pp. 2968 – 2973, Orlando, FL
20. A. Marthinsen (1999) Interpolation in Lie groups and homogeneous spaces. *SIAM J. Numer. Anal.*, 37:269–285
21. M. Mataric, M. Nilsson, K. Simsarian (1995) Cooperative multi-robot box pushing. In *IEEE/RSJ International Conf. on Intelligent Robots and Systems*, pp. 556–561, Pittsburgh, PA
22. C. R. McInnes (1995) Autonomous ring formation for a planar constellation of satellites. *AIAA Journal of Guidance Control and Dynamics*, 18:1215–1217
23. L. Noakes, G. Heinzinger, B. Paden (1989) Cubic splines on curved spaces. *IMA J. of Math. Control & Information*, 6:465–473
24. R. Olfati-Saber, R. M. Murray (2002) Distributed cooperative control of multiple vehicle formations using structural potential functions. In: *IFAC World Congress*, pp. 346–352, Barcelona, Spain
25. F. C. Park, B. Ravani (1994) Bezier curves on Riemannian manifolds and Lie groups with kinematics applications. *ASME Journal of Mechanical Design*, 117:36–40
26. W. H. Press, S. A. Teukolsky, W. T. Vetterling, B. P. Flannery (1998) *Numerical Recipes in C*. Cambridge University Press, Cambridge, UK
27. B. Roth (1981) Rigid and flexible frameworks. *American Mathematical Monthly*, 88:6–21
28. K. Shoemake (1985) Animating rotation with quaternion curves. *ACM Siggraph*, 19:245–254
29. T. R. Smith, H. Hanssmann, N. E. Leonard (2001) Orientation control of multiple underwater vehicles. In: *40th IEEE Conference on Decision and Control*, pp. 4598–4603, Orlando, FL
30. L. Srinivasan, Q. J. Ge (1998) Fine tuning of rational b-spline motions. *ASME Journal of Mechanical Design*, 120:46–51
31. T. Sugar, V. Kumar (2000) Control and coordination of multiple mobile robots in manipulation and material handling tasks. In: P. Corke and J. Trevelyan (eds.), *Experimental Robotics VI: Lecture Notes in Control and Information Sciences*, *vol.* 250, Springer, Berlin Heidelberg New York, pp. 15–24
32. P. Tabuada, G. J. Pappas, P. Lima (2001) Feasible formations of multi-agent systems. In: *American Control Conference*, Arlington, VA

33. Herbert G. Tanner, George J. Pappas, Vijay Kumar (2002) Input-to-state stability on formation graphs. In: *Proceedings of the IEEE International Conference on Decision and Control*, pp. 2439–2444, Las Vegas, NV
34. P. Varaiya (1993) Smart cars on smart roads: problems of control. *IEEE Transactions on Automatic Control*, 38:195–207
35. M. Žefran, V. Kumar (1998) Interpolation schemes for rigid body motions. *Computer-Aided Design*, 30:179–189
36. M. Žefran, V. Kumar, C. Croke (1995) On the generation of smooth three-dimensional rigid body motions. *IEEE Transactions on Robotics and Automation*, 14:579–589

# Part IX

# Reaching and Motion Planning